ELSEVIER

Surface Science 381 (1997) L551–L557

surface science

Surface Science Letters

Surface alloying and dealloying in Bi/Cu(001) at low coverage

H.L. Meyerheim [a,*], H. Zajonz [a], W. Moritz [a], I.K. Robinson [a,b]

[a] *Institut für Kristallographie and Angewandte Mineralogie der Universität München, Theresienstraße 41, 80333 München, Germany*
[b] *Department of Physics, University of Illinois, Urbana, IL 61801, USA*

Received 24 October 1996; accepted for publication 13 January 1997

Abstract

Using surface X-ray diffraction we have investigated the structure of the Bi/Cu surface alloy formed after Bi deposition on Cu(001) at room temperature. At low Bi coverage below about 0.35 ML (1 ML = 1.53×10^{15} atoms cm^{-2}), the intensity distribution along the integer order crystal truncation rods indicates surface alloying where Bi atoms substitute Cu surface atoms. The Bi atoms adsorb 0.61 (10) Å above the surface Cu layer. At a coverage above about 0.35 ML where the formation of a well-ordered c(2 × 2) superstructure starts to set in, we observe surface dealloying indicated by a rapid decrease of the fractional Cu occupancy of the surface layer with increasing Bi coverage. The Bi atoms are located in hollow sites at an adsorption height of 2.27 (10) Å corresponding to a hard sphere radius of 1.63 (8) Å, somewhat below the metallic radius of 1.82 Å. © 1997 Elsevier Science B.V.

Keywords: Bismuth; Copper; Surface structure; X-ray diffraction

It is well known that the solubility of the elements Pb and Bi in Cu is very limited (< 3 ppm at 600°C) and there exist no intermetallic compounds [1]. In spite of the impossibility of growing three-dimensional intermetallic compound crystals which can be attributed to the diffrerent metallic radii of the elements (Bi = 1.82 Å, Pb = 1.75 Å, Cu = 1.27 Å), two-dimensional alloying has been observed and investigated in a number of studies for different adsorbate–substrate combinations [2–9]. For example, using low energy electron diffraction (LEED), Gauthier et al. [3] determined a structural model for the c(4 × 4) phase of Pb on Cu(001) which consists of an ordered Pb/Cu alloy with alternating Cu and Pb close-packed chains. Using surface X-ray diffraction (SXRD) a Bi chain substituting Cu substrate atoms has also been found to be the main characteristic for the p(4 × 1) superstructure of the Bi/Cu(110) reconstruction [4]. Whereas these recent investigations and a number of previous ones [5–9] focused on the analysis of ordered structures, information at low adsorbate coverages where no ordered superstructures are formed is rare. In a recent scanning tunneling microscopy (STM) work on Pb/Cu(111), Nagl et al. [10] observed surface alloying at low Pb coverage and dealloying above a maximum packing density of about 40% of a close-packed Pb overlayer. In the following the term "dealloying" means the reversal of the alloying process, i.e. a reduction of the concentration of substitutional adatom sites and the formation of an adatom structure on the (unaltered) substrate surface.

For room temperature adsorption of Bi on

* Corresponding author. Fax: +49 89 2394 4334; e-mail: uk40104@sunmail.lrz-muenchen.de

PII S0039-6028(97)00052-6

Cu(001) several LEED investigations have been performed so far [11–13], reporting the formation of different ordered superstructures. With increasing Bi coverage, Delamare and Rhead [11] found a p(2×2) and a c(2×2) superstructure, as well as two superstructures whose diffraction patterns were indexed as a c($9\sqrt{2}\times\sqrt{2}$) and a p($\sqrt{41}\times\sqrt{41}$) superstructure. In this context it should be noted that the p(2×2) structure could not be prepared in a later investigation [13] as well as in our experiments. For all adsorbate phases reported by Delamare and Rhead [11], structural models were proposed; however, a detailed investigation is lacking so far. Moreover, for the coverage regime $\Theta \ll 0.50$ ML, where only the (1×1) symmetry of the Cu(001) surface can be observed, nothing is known about the local adsorption geometry of the Bi atoms. As has been shown in the past, SXRD is well suited to the analysis of local adsorption geometries by monitoring the integer-order crystal truncation rods (CTRs) [14,15]. In the present investigation we therefore focus on the structure analysis of the local Bi adsorption geometry at low coverage; a detailed investigation of the ordered superstructures will be published elsewhere [16].

The X-ray experiments were performed using an 18 kW rotating anode X-ray generator and a sagittally focusing pyrolytic graphite monochromator selecting Cu Kα radiation. The Cu(001) crystal ($\varnothing \approx 10$ mm) was cleaned by standard procedures until no traces of contaminants could be detected by Auger electron spectroscopy (AES). High sample surface quality was obtained in this way as checked by SXRD. The full width at half maximum (FWHM) at the (10L) antiphase condition along the (10L) rod was 0.22° which is the resolution limit of our diffractometer. We use a sample setting corresponding to a primitive (1×1) surface unit cell, therefore the a-, b- and c-axis of the surface unit cell is parallel to [110], [1$\bar{1}$0] and [001] of the bulk fcc unit cell.

Highly purified Bi (6N) was deposited from a water-cooled Knudsen cell placed about 15 cm from the sample. Heating the Knudsen cell to about 540°C resulted in a deposition rate of about 0.05 ML Bi per minute. The coverage is expressed as the number of Bi atoms relative to the number of surface Cu atoms so that 1 ML equals 1.53×10^{15} atoms·cm^{-2}. Since there is one Cu atom in the primitive (1×1) unit cell the term "fractional Bi coverage" (θ_{Bi}, see below) is identical with the Bi coverage as expressed in ML of Cu. Fig. 1a shows as solid triangles and circles the measured peak-to-peak intensities of the Bi (96 eV) and the Cu (60 eV) Auger transitions versus Bi deposition time. The lines are guides to

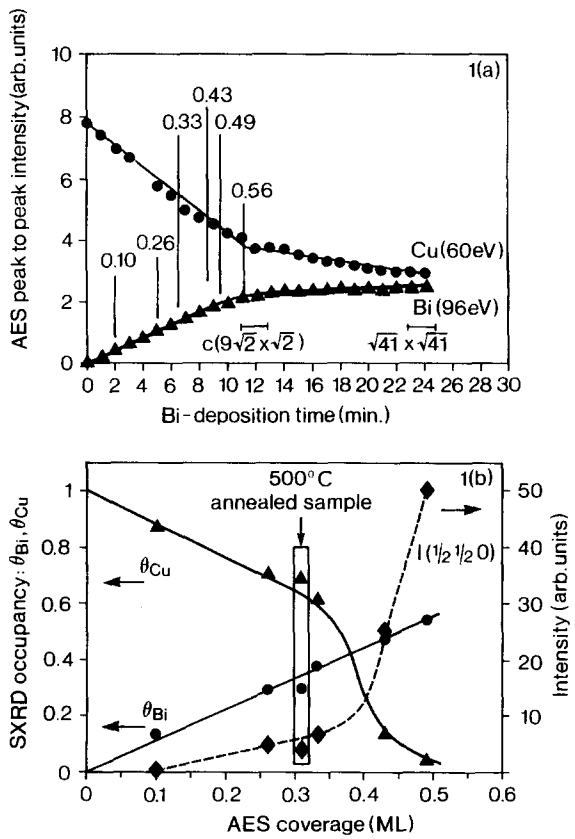

Fig. 1. (a) Auger peak-to-peak intensities for the Bi 96 eV and the Cu 60 eV transitions as a function of Bi deposition time. The solid lines are guides to the eye. Surface X-ray diffraction data were collected after 2.0, 5.0, 6.5, 8.5, and 9.5 min as well as after annealing the 6.5 min sample. The corresponding Bi coverages (in ML) are indicated at the vertical lines. The calibration is based on the appearance of the c($9\sqrt{2}\times\sqrt{2}$) phase corresponding to 0.56 ML Bi coverage. (b) SXRD derived fractional Bi occupancy (filled circles) and top-layer Cu occupancy (triangles) as a function of the AES-calibrated Bi coverage. The diamonds indicate the integral intensity of the (1/2 1/2 0) reflection. The data in the frame correspond to the 500°C annealed sample. Lines are guides to the eye.

the eye. After a linear increase there is a sudden change in slope after about 11 min which coincides with the formation of the c($9\sqrt{2}\times\sqrt{2}$) phase. The structure indexed as p($\sqrt{41}\times\sqrt{41}$) in Ref. [11] appears after about 20–24 min. Using a Bi coverage of 0.56 ML for the c($9\sqrt{2}\times\sqrt{2}$) phase formed after 11 min deposition [16], a Bi coverage calibration is possible using the AES data. It should be noted in advance that on the basis of our SXRD data, both the c($9\sqrt{2}\times\sqrt{2}$) and the ($\sqrt{41}\times\sqrt{41}$) phase can be regarded as "antiphase domain" structures basically very similar to the c ($5\sqrt{2}\times\sqrt{2}$) structure discussed in Ref. [6]. Further, the ($\sqrt{41}\times\sqrt{41}$) structure is better described by a c(10×10) structure.

The SXRD data discussed in the following were collected after five different depositions (2.0, 5.0, 6.5, 8.5, and 9.5 min) as shown by the vertical lines in Fig. 1a. According to the AES calibration the depositions correspond to Bi coverages (ML) which are given by the numbers. A sixth data set was taken after annealing the 6.5 min sample at 500°C for 5 min. For each preparation the (10L), (11L) and the (21L) truncation rods were measured in steps of $\Delta q_z = 0.05$ reciprocal lattice units (rlu). As an example we show in Fig. 2 as solid circles the measured structure factor intensities, $|F|^2$, for the 500°C annealed sample. Each data point represents an integrated intensity measured by rotating the the sample around the surface normal under total reflection conditions of the incident beam [17]. A maximum normal momentum transfer q_z of two reciprocal lattice rods (rlu) corresponding to 3.48 $Å^{-1}$ could by achieved for the (10L) and the (11L) rods. In this way one data set contains about 80–90 symmetry-independent reflections. We used Soller slits with 0.8° angular width in front of the detector leading to an out-of-plane resolution of $5.69\times10^{-2}\cos(\alpha_f)$ $Å^{-1}$. This corresponds to about 0.032 rlu for in-plane measurements ($\alpha_f \approx 0$), where α_f represents the beam exit angle. In Fig. 2 the solid lines show the best fits to the data, for all data sets the weighted residuals (R_w) were in the range between 0.039 and 0.057 which can be regarded as very good. This is also expressed by the goodness of fit (GOF) parameter [17] which is in the range between about 0.8 and 1. Apart from a scale factor the fractional

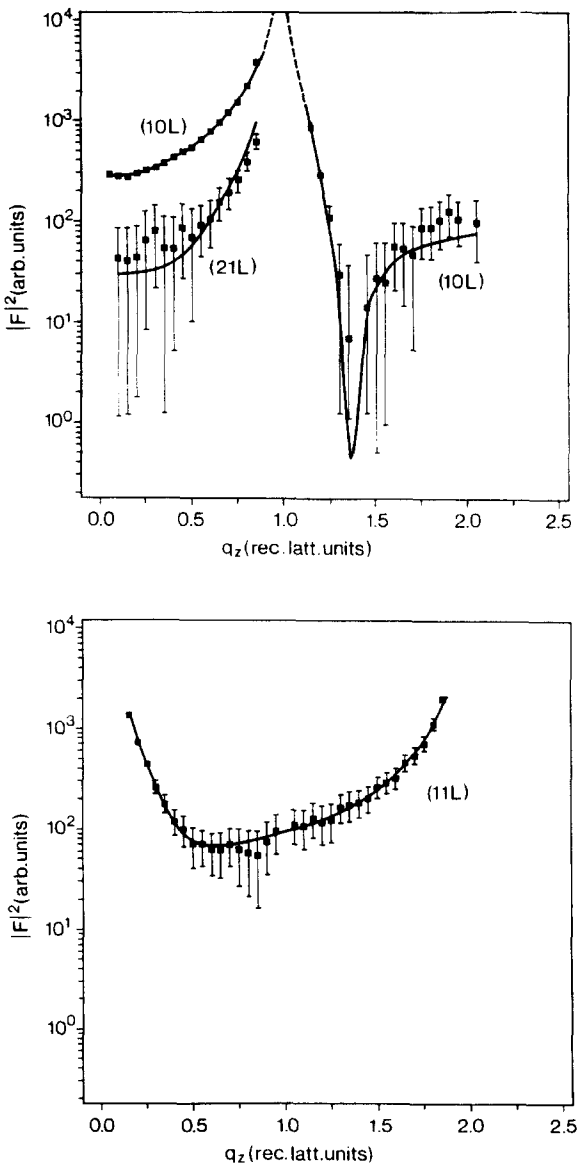

Fig. 2. Measured (squares) and calculated (solid lines) structure factor intensities, $|F|^2$, along the (10L), (21L) and the (11L) crystal truncation rods for the 500°C annealed sample.

occupancies of Bi and Cu in the first layer (θ_{Bi}, θ_{Cu}) and the positional parameters were refined. Due to the 4 mm site symmetry of the Bi atom on the Cu(001) surface in substitutional and in hollow site position (see below), only the z-components of the Bi and top layer Cu atoms can be varied. Taking account of deeper Cu layers did

not lead to any improvement. We also fitted the Bi disorder as expressed by the Debye parameter $B=8\pi\langle u^2\rangle$, where $\langle u^2\rangle$ is the (isotropic) mean-square displacement. At low coverages the Bi atoms were found to occupy the substitutional site, in this way statistically replacing top-layer Cu atoms as shown schematically in Fig. 3a. The Bi atoms are shown as filled circles; Cu atoms are shown as open circles. Within the primitive (1×1) unit cell (indicated by the square) the substitutional site corresponds to the position $(00z)$. The refined fractional occupancies of the first-layer Cu atoms and the Bi atoms are shown in Fig. 1b as a function of the AES coverage. The integrated intensities of the fractional order $(1/2\ 1/2\ 0)$ reflections measured for the different coverages are indicated by the diamonds. An intensity different from zero indicates the presence of some $c(2\times2)$ long-range order (LRO). Several results can be summarized:

(i) There is a linear increase of the refined Bi occupancy with deposition time. Within an error bar of about 0.03–0.05 for θ_{Bi} there is a good agreement between the AES and the SXRD-derived coverage.

(ii) At coverages below about 0.35 ML the relation $\Theta=\theta_{Bi}+\theta_{Cu}\approx1$ for the total occupancy of the surface layer (Θ) holds, i.e. there are no significant vacancies within the surface layer. It should be emphasized that in most cases both fractional occupancies could be refined simultaneously. Above about $\theta_{Bi}=0.35$ we observe a rapid decrease of θ_{Cu} which can be interpreted by surface dealloying. Further, the formation of a well-ordered $c(2\times2)$ phase starts to set in. This is evident by the rapid increase in the superlattice reflection intensity.

(iii) The dealloying process is finished after about 8.5–9.5 min Bi deposition time (0.43–0.49 ML), where we determine a top-layer Cu occupancy close to zero and a well-defined $c(2\times2)$ superstructure. Apart from the high $(1/2\ 1/2\ 0)$ reflection intensity, this can be deduced by the full width at half maximum (FWHM) of the reflection profile which at the highest coverage equals to 3.39×10^{-3} rlu. For comparison, the reflections measured below 0.35 ML are more than three times as wide.

(iv) Annealing the Bi deposited Cu surface for

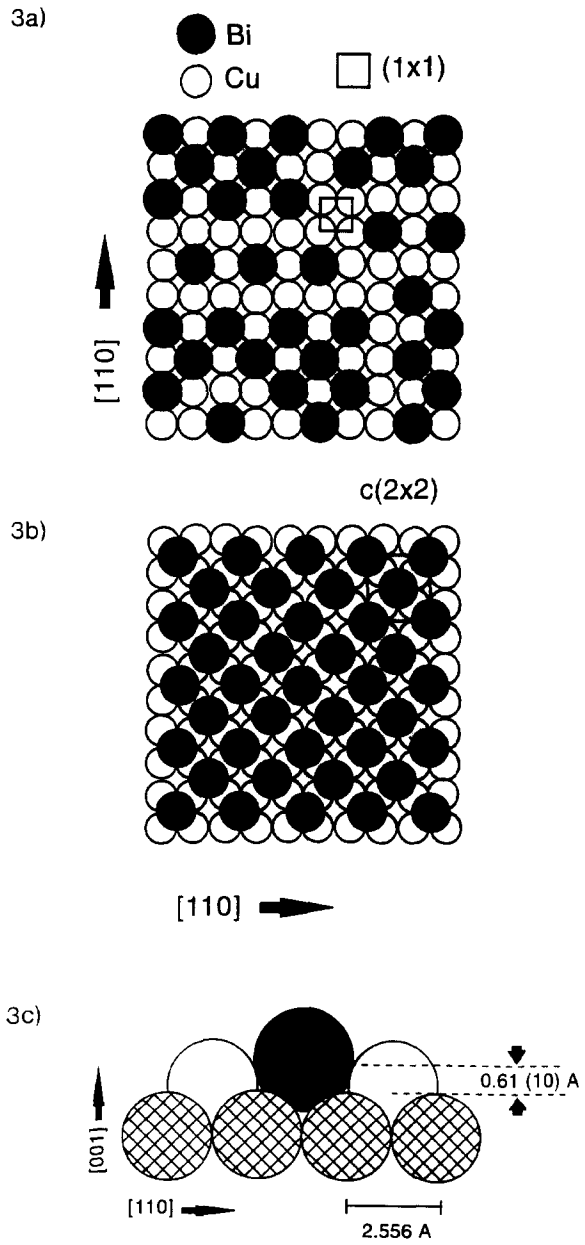

Fig. 3. (a) Structure model for the Bi/Cu surface alloy shown schematically in top view for $\theta_{Bi}=0.34$, i.e. close to the beginning of the dealloying. The Bi atoms are represented as filled circles, Cu atoms as open circles. The primitive (1×1) surface unit cell is indicated by the square. The direction indices are related to the bulk fcc setting. (b) Structure of the ideal Bi/Cu(001) $c(2\times2)$ superstructure. The $c(2\times2)$ superlattice cell is indicated by the square. (c) Side view of the substitutional Bi geometry. Bi adsorbs 0.61 (10) Å above the first-layer Cu atoms. Second-layer Cu atoms are shown hatched.

5 min at 500°C (such as, e.g., the 0.33 ML sample) leads to a partial reversal of the alloying process, probably due to some evaporation of Bi. For this sample we find $\theta_{Bi}=0.30$ (3) and $\theta_{Cu}=0.70$ (3) as shown by the data in the frame of Fig. 1b. The substitutional geometry is still preserved, indicating that it is the thermodynamically most stable configuration of Bi on Cu(001) at this coverage.

(v) Considerable coverage-dependent disorder is observed for the Bi atoms as expressed by the Debye parameter B. At low ($\theta_{Bi}=0.10$) and high ($\theta_{Bi}>0.35$) coverage it is in the range of about 4 Å^2 ($\langle u^2\rangle=0.05$ Å^2); however at intermediate coverages (datasets taken at 0.26 and 0.33 ML as well as after annealing the 0.33 ML sample at 500°C) we determine $B\approx 10$ Å^2 ($\langle u^2\rangle=0.13$ Å^2). Thus, the maximum of the Bi disorder lies in the regime close to the beginning of the dealloying; consequently, the coverage dependence might be attributed to steric reasons. In contrast, no such disorder is observed for the top Cu layer, whose B factor was kept constant at 0.6 Å^2. Finally, we derive a 3–4% expansion of the first Cu interlayer spacing relative to the bulk spacing ($\Delta d_{12}/d_{bulk}$), however, this needs a caveat, since the error bar for this parameter is in the range of 100% due to the dominant contribution of Bi scattering in the (simultaneous) refinement.

(vi) For all data sets the roughness factor β as described by Robinson [14] was also refined. In general we determined values in the regime between 0.05 and 0.10 which can be considered as quite low for metal surfaces.

In total, 7–8 free parameters (including the overall scale factor) were used to describe the surface structure which is in a reasonable relation with the number of reflections ($N=70$–80). It should again be emphasized that the fits of the data are very good for all data sets. One representative example (500°C annealed sample) is shown in Fig. 2. Assuming different structral models such as, e.g., hollow, bridge or top site adsorption on the unaltered Cu(001) surface, we obtained significantly worse fits as expressed by the weighted residual R_w which is in the 0.20 regime for these cases. Consequently, the structural model developed so far can be considered as highly reliable. For the discussion of the results we focus on Figs. 3a,b which show the alloy structure with $\theta_{Bi}=0.34$ and the perfect c(2×2) superstructure, respectively. The occupancy $\theta_{Bi}=0.34$ is close to the beginning of the dealloying process. From this picture our SXRD results can be explained quantitatively. Up to a coverage around 0.35 ML, Bi atoms can substitute Cu atoms on the Cu(001) surface and simultaneously avoid a local configuration with two Bi atoms as nearest neighbours (NN) along ⟨110⟩. From the larger size of the Bi atoms in comparison with the Cu atoms ($r_{Bi}=1.63$ (8) Å derived from the SXRD data, compared to $r_{Cu}=1.27$ Å, see below) it is reasonable to assume a Bi configuration with Bi–NN pairs only along the ⟨100⟩ directions. This picture is in line with Tersoff's recent calculations [18], showing that surface alloy formation can generally be expected in systems with a large size mismatch and that second NN occupation is energetically favorable for alloying (001) surfaces. We emphasize that there is no direct evidence for this assumption, however. If we assume this packing rule, then some c(2×2) short-range order will necessarily be generated, as Fig. 3a ($\theta_{Bi}=0.34$) shows. It is therefore understandable that c(2×2) LRO is observed by the appearance of the (1/2 1/2 0) reflection around 0.3 ML. Finally, Fig. 3c shows a side view of the substitutional geometry. After the dealloying process stops, the Bi atoms reside in four-fold hollow sites at an adsorption height of 2.27 (10) Å. What was previously the second layer of the alloy system can now be considered to be the Cu(001) surface. Using the simple hard sphere model and a Cu radius of 1.27 Å, an effective Bi radius of 1.63 (8) Å is derived which is about 10% lower than the metallic Bi radius.

The CTR data for the (dealloyed) c(2×2) structure discussed so far can be compared with the analysis of a full data set consisting of both CTR and superlattice rods leading to 114 independent reflections in total [16]. This data set was taken from a c(2×2) superstructure which was prepared by deposition of a large amount of Bi (≥1 ML) and subsequent annealing at 500°C for 5 min. The Bi atoms occupy the hollow site at 2.18 (8) Å above the surface and a contraction of the first Cu interlayer spacing by 1.5% is observed. We do not consider the differences between the Bi adsorption

heights derived from both samples as very significant. However, from the full data set we have some evidence for Bi also to occupy with about a 5–10% probability the remaining hollow sites of the c(2 × 2) structure, i.e. in the positions (1/2, 0, z) and (0, 1/2, z) of the c(2 × 2) unit cell shown in Fig. 3b. Due to steric reasons not all Bi sites of the c(2 × 2) structure can be occupied simultaneously. Reducing the Bi occupancy at (00z) and (1/2, 1/2, z) to about 90% yields a better fit with the data than the ideal c(2 × 2) structure model ($R_w = 0.08$ compared with $R_w = 0.13$). The additional adatoms are attributed to Bi, since the derived adsorption height is 2.33 (12) Å which is not compatible with Cu adsorption. This "defect structure" is not observed for the sample series discussed here which might be attributed to the different preparations.

In summary, we have analysed the structural evolution of the Bi/Cu(001) interface at room temperature. Our SXRD data indicate the formation of a disordered Bi/Cu surface alloy up to a coverage of about 0.35 ML. Increasing the Bi coverage leads to surface dealloying and the formation of a well-ordered c(2 × 2) Bi/Cu(001) superstructure at 0.50 ML. In order to account for the mechanisms responsible for the alloying, apart from atomic size arguments structural and electronic reasons can also be discussed. First, substitutional site adsorption leads to an increase in the adatom coordination and to a shielding of the repulsive dipole–dipole interaction such as is observed for alkali adsorption [19]. Both factors are found to contribute to an adsorption energy gain necessary to overcome the energy cost to remove substrate surface atoms [20]. However, the shielding of the dipole interaction might be less important here since the Bi adsorption was found to be much less ionic then alkali adsorption as judged from work function measurements [21]. On the other hand an important contribution appears to come from the Bi induced surface charge redistribution which was investigated by helium scattering at low Bi and Pb coverages [22]. For both adsorbate species it is suggested that the surface charge redistribution which makes the charge density of the Cu atoms more atomic like and localized than for the clean surface, leads to a weakening of the surface Cu–Cu bonds. In this way a lowering of the energy barrier for removing a surface Cu atom and subsequent alloy formation can be inferred. Comparing the adsorption structures formed by Bi and Pb (size difference 4%) on Cu(001) [3,6] some basic similarities are evident, although differences exist in detail. For Pb/Cu(001) an ordered alloy structure is observed for the c(4 × 4) phase at a Pb coverage of 0.375 ML. With increasing coverage, dealloying takes place and Pb atoms are located in hollow sites for the c(2 × 2) phase at 0.5 ML and/or are arranged in c(2 × 2) antiphase domains as determined for the c($5\sqrt{2} \times \sqrt{2}$) superstructure at 0.6 ML. The latter superstructures are similar to those determined for the Bi/Cu(001) system [16]; however, an ordered alloy at low coverage has not been found in our investigation. From the crystallochemical point of view Bi and Pb adsorption on Cu(001) can be seen as a limiting case where a large size mismatch with Cu (Bi = 43%, Pb = 38%) leads to complete dealloying at high coverage. This is in contrast to the Pd/Cu(001) system (mismatch only 8%), where no dealloying for the c(2 × 2) structure is observed [23].

Acknowledgements

The authors would like to thank J.J. Csiszar for maintenance of the rotating anode X-ray source and R. Wunderlich for preparing the figures. The help of D. Wolf and the workshop staff during the experiments is gratefully acknowledged. I.K. Robinson acknowledges the hospitality of the SFB 338 during an extended visit in Munich.

References

[1] D.J. Chakraborti, R.E. Laughlin, Bull. Alloy Phase Diag. 5 (1984) 148.
[2] U. Bardi, Rep. Prog. Phys. 57 (1994) 939.
[3] Y. Gauthier, W. Moritz, W. Hösler, Surf. Sci. 345 (1996) 53.
[4] L. Lottermoser, T. Buslaps, R.L. Johnson, R. Feidenhans'l, M. Nielsen, D. Smilgies, E. Landemark, H.L. Meyerheim, Surf. Sci., to be published.
[5] A. Sepulveda, G.E. Rhead, Surf. Sci. 66 (1972) 436.
[6] W. Hösler, W. Moritz, Surf. Sci. 117 (1982) 196.

[7] M. Paffet, C.T. Campbell, T.N. Taylor, J. Chem. Phys. 85 (1986) 6176.
[8] W.D. Clendening, C.T. Campbell, J. Chem. Phys. 90 (1989) 6656.
[9] D.C. Godfrey, B.E. Hayden, A.J. Murray, R. Parsons, D.J. Pegg, Surf. Sci. 294 (1993) 33.
[10] C. Nagl, O. Haller, E. Platzgummer, M. Schmid, P. Varga, Surf. Sci. 321 (1994) 237.
[11] F. Delamare, G.E. Rhead, Surf. Sci. 35 (1973) 172.
[12] B. Blum, E.W. Plummer, H.L. Davis, D.M. Zehner, J. Vac. Sci. Technol. A9 (1991) 1703.
[13] C. Argile, G.E. Rhead, Surf. Sci. 78 (1978) 115.
[14] I.K. Robinson, Phys. Rev. B 33 (1986) 3830.
[15] H.L. Meyerheim, J. Wever, V. Jahns, W. Moritz, P.J. Eng, I.K. Robinson, Surf. Sci. 304 (1994) 267.
[16] H.L. Meyerheim, W. Moritz, M. DeSantis, I.K. Robinson, unpublished.
[17] I.K. Robinson, in: Handbook of Synchrotron Radiation, Eds. D.E. Moncton, G.S. Brown, Vol. 3 (North-Holland, Amsterdam, 1990).
[18] J. Tersoff, Phys. Rev. Lett. 74 (1995) 434.
[19] R. Fasel, P. Aebi, J. Osterwalder, R.G. Agostino, G. Chiarello, Phys. Rev. B 50 (1994) 14516.
[20] C. Stampfl, J. Neugebauer, M. Scheffler, Surf. Rev. Lett. 1 (1994) 213.
[21] M.T. Paffet, C.T. Campbell, T.N. Taylor, J. Chem Phys. 85 (1986) 6176.
[22] W. Li, G. Vidali, Surf. Sci. 287/288 (1993) 336.
[23] P.W. Murray, I. Stensgaard, E. Stensgaard, E. Lægsgaard, F. Besenbacher, Surf. Sci. 365 (1996) 591.